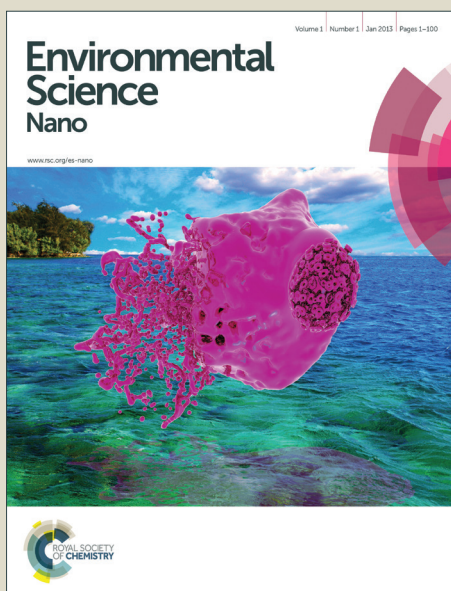


Environmental Science Nano

Accepted Manuscript



This is an *Accepted Manuscript*, which has been through the Royal Society of Chemistry peer review process and has been accepted for publication.

Accepted Manuscripts are published online shortly after acceptance, before technical editing, formatting and proof reading. Using this free service, authors can make their results available to the community, in citable form, before we publish the edited article. We will replace this *Accepted Manuscript* with the edited and formatted *Advance Article* as soon as it is available.

You can find more information about *Accepted Manuscripts* in the [Information for Authors](#).

Please note that technical editing may introduce minor changes to the text and/or graphics, which may alter content. The journal's standard [Terms & Conditions](#) and the [Ethical guidelines](#) still apply. In no event shall the Royal Society of Chemistry be held responsible for any errors or omissions in this *Accepted Manuscript* or any consequences arising from the use of any information it contains.

NANO IMPACT STATEMENT**Exploring Controls on the Fate of PVP-capped Silver Nanoparticles in Primary Wastewater Treatment**

Stephen M. King^a, Helen P. Jarvie, Michael J. Bowes,
Emma Gozzard, Alan J. Lawlor and M. Jayne Lawrence

ISIS Facility, STFC Rutherford Appleton Laboratory, Harwell Oxford
Didcot, OX11 0QX, United Kingdom, *Corresponding author*,
Tel: +44 (0)1235 446437; e-mail: stephen.king@stfc.ac.uk

The sources, transport, and fate of silver nanoparticles (AgNPs) are of concern due to the chemical toxicity of silver to microbes and algae. The greatest source of AgNPs to the environment is via wastewater discharges, meaning there is a potential risk to the microbial biofilms in secondary wastewater treatment. This study explores the behaviour of AgNPs in primary wastewater treatment, primarily using small-angle neutron scattering. The results show that AgNPs coated in a non-ionic stabiliser (PVP) undergo rapid settling in wastewater and will be removed to sewage sludge, rather than continuing to the secondary treatment stage. This settling behaviour seems to be controlled by hitherto unexplored synergistic interactions between hydrophilic parts of the non-ionic stabiliser and anionic components in the wastewater and is therefore generic.

ARTICLE

Exploring Controls on the Fate of PVP-Capped Silver Nanoparticles in Primary Wastewater Treatment

Cite this: DOI: 10.1039/x0xx00000x

Stephen M. King^{a*}, Helen P. Jarvie^b, Michael J. Bowes^b, Emma Gozzard^b, Alan J. Lawlor^c and M. Jayne Lawrence^dReceived 00th January 2012,
Accepted 00th January 2012

DOI: 10.1039/x0xx00000x

www.rsc.org/

Small-angle neutron scattering has been used to examine the settling behaviour of partially-passivated silver nanoparticles (AgNP), capped with a polyvinylpyrrolidone (PVP) stabiliser, in water and domestic wastewater, in a primary clarification 'microcosm' as a function of time. The impact of two flocculants routinely used in the wastewater treatment process has also been studied. The settling velocity is found to be time-dependent, but always exceeds 100 mm hr⁻¹ during the first hour at the point of input. Particle removal by settling is almost three times greater in wastewater than it is in pure water. The results are rationalised in terms of a generic, but synergistic, interaction between non-ionic capping agents and anionic components of wastewater, and we show how this may afford an explanation for some of the diversity of behaviour previously reported in studies of several different NPs in wastewater treatment. We conclude that AgNPs entering primary clarification with non-ionic surface coatings, whether present by design or environmental transformation, pose no threat to the viability of the biofilms in secondary wastewater treatment.

Introduction

Background. Humankind's appetite for engineered nanomaterials, ENMs, (ie, *excluding* the commodity nanomaterials carbon black and pyrogenic/fume silica which account for >96% of overall production) has recently been estimated at around 0.4 Mt yr⁻¹ representing, by the time this paper is published, a market worth some €3 bn (\$4 bn).^{1,2,3,4} Roughly two-thirds of all ENMs produced are metal oxide nanoparticles (eg, aluminium oxide, barium titanate, cerium oxide, iron oxide, titanium dioxide, zinc oxide).^{4,5,6,7} Pure metal nanoparticles (eg, copper, gold, palladium, platinum, ruthenium, silver) currently account for <1% of ENM production but this is predicted to rise, particularly with advances in catalysis and an increasing number of applications in healthcare and the electronics industry. Indeed, in the last decade, worldwide demand for silver nanoparticles (AgNPs), the subject of this study, is estimated to have increased from <10 t yr⁻¹ to over 300 t yr⁻¹ (~1% of all silver produced).^{5,8,9,10,11}

AgNPs have found a multitude of uses; in recent history in the photographic industry, nowadays as anticorrosive pigments for primers and coatings, in conductive inks and flexible touch screens, but most notably in portable water purification, food packaging, high-performance clothing, wound dressings, and some medical devices, along with other less mainstream consumer health products.^{8,11,12} This is because silver has long been known to be a potent, broad-spectrum, bactericide. It is also an effective viricide, algacide and fungicide. The presence of AgNPs in these products, rather than bulk silver, aids fabrication, lowers costs, and conveys greater efficacy. The problem, of course, is that at any point in the

lifecycle of these products the AgNPs may be released to the environment, whether by accidental release during manufacture, through abrasion or cleaning during use, or after degradation of the matrix following disposal.^{13,14} The challenges for environmental nanoscience and (nano-)ecotoxicology are then: where do the AgNPs go, in what concentrations, what happens to them, and what are the consequences?^{15,16,17,18}

For a large proportion of manufactured NPs, not just AgNPs, their major route of release into the natural environment is via sewage and industrial wastewater discharges, and from urban drainage.¹⁹ This means our wastewater treatment plants (WWTP) unwittingly act as 'gateways', controlling release of NPs and their transformation products from domestic and industrial sources to the aquatic or terrestrial environments: either via the treated effluent which is discharged into surface waters or, via sewage sludge disposal to land.^{20,21,22} AgNPs (and CuNPs too) are of particular concern to the wastewater treatment industry because these biocidal NPs pose a threat to the viability of the mixed microbial communities in the biofilms present in secondary wastewater treatment.^{23,24,25,26,27,28}

Those biofilms break down organic pollutants (eg, organic chemicals, drug metabolites, etc) in the effluent received from primary treatment and are critical to the final quality of the treated discharge. Without the biofilms the aquatic environment would be further impacted. Thus the efficacy of primary wastewater treatment at removing harmful NPs, and the chemical transformation of NPs throughout wastewater treatment more generally, become key considerations.

References 23-28 show that whilst ionic (dissolved) silver is most toxic to the microbes, nanoparticulate silver also has some toxicity.

What is less clear, however, is whether that toxicity is due to the AgNPs themselves (or their surface coatings), and/or because they promote the formation of reactive oxygen species (ROS). The dissolution of coated AgNPs has been shown to be inversely related to size^{29,30}, water hardness, pH, and NOM (natural organic matter) concentration³¹, but also directly related to DOC (dissolved organic carbon) concentration³². However, it has also been shown that humic acids (a form of NOM) can reduce silver ions under environmentally relevant conditions to form non-anthropogenic AgNPs.³³ Another key process is sulphidation of the AgNP to form Ag₂S^{34,35,36}. In the case of AgNPs this oxidative dissolution process *retards* the release of silver ions (in contrast, it promotes the release of copper ions from CuNPs³⁷) but is, again, also strongly size-dependent (smaller particles being transformed more).

Previous work. There are now several published studies on the fate and behaviour (as distinct from the application) of NPs in wastewater treatment, split between those that report on NP interactions with wastewater, and those that are concerned with NPs in the sludge (biosolids). Here we are primarily concerned with the former.

Chang *et al*³⁸ looked at the coagulation of *silica* NPs in the effluent from a semiconductor chemical-mechanical planarization plant by polyaluminium chloride. These NPs would almost certainly have carried adsorbed surfactant coatings but there is no information on what the surfactants were. NP removal to the sewage sludge was found to be minimal. Jarvie *et al* have also studied the behaviour of *silica* NPs, both uncoated (uncapped) and coated (capped; with a nonionic surfactant), in real municipal wastewater but in a laboratory model settlement tank.³⁹ In contrast to Chang *et al*, the uncoated NPs were found to be quite stable, remaining in dispersion, but the coated NPs rapidly agglomerated and settled. From this they inferred that there must have been a specific interaction between the surfactant coating and components of the wastewater. Limbach *et al*⁴⁰ studied the agglomeration of both uncoated and coated (with an anionic surfactant or anionic polymer) *ceria* NPs in a laboratory model WWTP. Though the majority of NPs were eventually removed to the sewage sludge these authors also noted the significant influence that the particle coatings could have on the process, highlighting “*complex interactions between dissolved species and the nanoparticles*”. Kiser *et al*⁴¹, Westerhoff *et al*⁴² and Wang *et al*⁴³ have investigated the fluxes of titanium entering and leaving some commercial WWTPs in the Southwest US, and conducted laboratory studies with uncoated *titania* NPs in a model WWTP. Again, the majority (~70–90%), but not all, of the NPs were removed to the sewage sludge. More recently, Lombi *et al*⁴⁴ have looked at the chemical stability of *zinc oxide* NPs (two uncoated, one coated with nonionic caprylic/capric triglycerides) in a laboratory model anaerobic digester (ie, they had already assumed these NPs would be removed to the sewage sludge at the primary treatment stage). All three types of NP were converted to the sulphide, but the transformation of the coated particles was found to be substantially retarded relative to the uncoated NPs. Ma *et al*³⁶ also examined the fate of *zinc oxide* NPs, this time uncoated, added to the primary sludge and the activated sludge basin in a pilot WWTP. The study concluded that the NPs were significantly chemically transformed during treatment, seemingly corroborating the findings of Lombi *et al*.

Fewer studies have concentrated on *metallic* NPs in wastewater. Kaegi *et al*⁴⁵ have investigated the behaviour of AgNP coated with a non-ionic surfactant in a pilot WWTP fed from a municipal source. More than 85% of the AgNP were determined to have been removed to the sewage sludge. However, the authors also highlighted a rapid (~2 hours) and substantial (~60–90%) transformation of the AgNPs into Ag₂S under increasingly anaerobic conditions. They also noted a

residual ~10% of AgNPs that either transformed much more slowly or not at all. This was ascribed to the protective effects of the surface coating and/or passivated particle surfaces. In their work, Ma *et al*³⁶ also studied AgNPs but coated with non-ionic polymer (poly(vinyl pyrrolidone), PVP). However, the fate of these AgNPs was the same as that of their zinc oxide NPs, suggesting that, in contrast, the surface coating offered little or no protection against sulphidation. However, this work was performed on samples that had been allowed to ‘age’ for a much longer length of time. In a more recent study, Kaegi *et al*⁴⁵ have extended their work to encompass the whole wastewater system. AgNPs coated with non-ionic surfactant were actually dosed into a trunk sewer, whilst AgNPs coated with PVP, or capped with citrate, were added to wastewater samples extracted from the sewer. The results demonstrated that AgNPs discharged to the sewer network are very likely to be efficiently delivered to the WWTP with only partial transformation. This was ascribed to the greater surface area for interaction presented by suspended sediment particles than by the sewer biofilms (which control the extent of sulphidation/enroument), rather than to a difference in binding affinity. AgNP removal efficiency in the wastewater experiments was very high (~99%) irrespective of the particle size or surface coating. Impellitteri *et al*⁴⁶ and Doolette *et al*⁴⁷ have also investigated the fate of PVP-coated AgNPs at the primary treatment stage. The former study reports over 97% of the AgNPs as being removed to the sludge. Both studies identify sulphidation as the dominant transformation once the AgNPs are in the sludge. In their study, Wang *et al*⁴³ also looked at carboxy-terminated (ie, anionic) polymer coated AgNP and found that whilst removal efficiency was less than for titania NPs, 88% of AgNPs were still removed to the sewage sludge. In contrast, Hou *et al*⁴⁸ studied citrate-capped (ie, anionic) AgNPs in a laboratory model WWTP and found that over 90% would pass through primary treatment. Though Tejamaya *et al*⁴⁹ have reported instability in dispersions of citrate-capped AgNPs, this was in a standard OECD toxicology test media, not wastewater. The organic makeup, ion composition, ionic strength and pH of the two media are rather different (compare Tables S1 and S2 in Reference 49 with the present Table S5). Very recently Johnson *et al*⁵⁰ have measured the total fluxes of silver entering and leaving nine commercial WWTPs, of three different process types, in the UK. For silver particles between 2–450 nm in size (ie, the filter fraction including AgNP’s) around 50% were found to be removed to the sewage sludge.

Thus, with one or two exceptions, the literature would appear to indicate that oxide/metallic NPs will usually be removed to the sewage sludge at the primary clarification stage of wastewater treatment. However, the efficiency of removal, and the extent of any chemical transformation, of the NPs would appear to be strongly influenced by the nature (eg, how attached, thickness, charge) of any surface coating, how that interacts with other species present in wastewater, the specific environmental conditions (eg, aerobic vs anaerobic), and the duration of exposure to the environment.

Present work. Against this background, in this work we have systematically explored the behaviour of one type of AgNP, coated with the *non-ionic* polymeric stabiliser PVP, in five different aqueous matrices: pure water, untreated wastewater (sewage), wastewater dosed with ferric chloride, and pure water dosed with two very different concentrations of the *anionic* polymer poly(sodium 4-styrene sulphonate), PSS. Ferric chloride and PSS are sometimes used as flocculants in industrial wastewater treatment to enhance clarification (solids removal), a process known as advanced primary treatment. Ferric chloride may also be used in a tertiary treatment stage designed to strip phosphorus from the effluent. Thus our study covers the gamut of chemical conditions that the AgNPs are

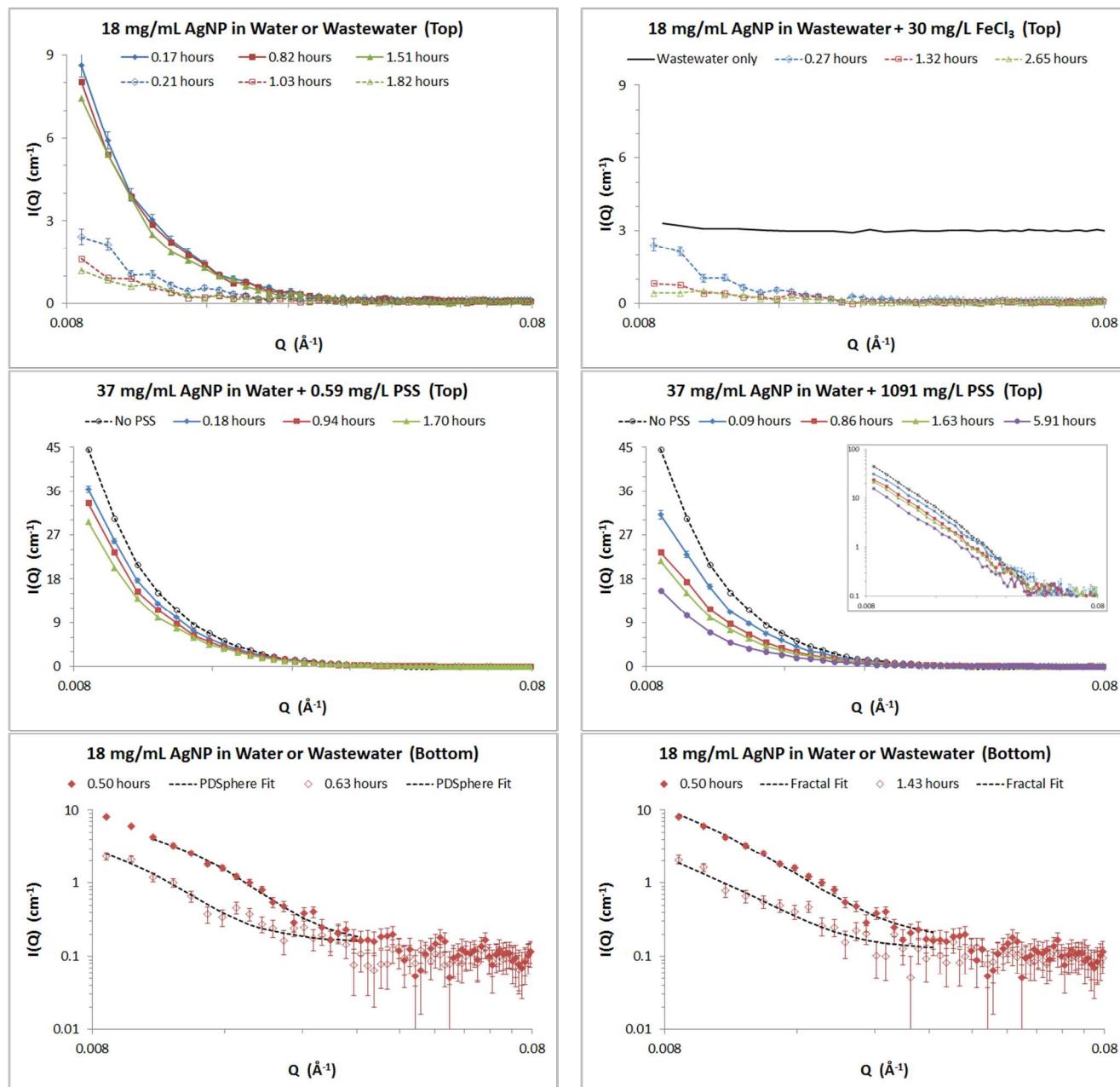


Figure 1: Example SANS data at different times from: (top left pane) 18 mg/mL AgNP in nanopure water (filled symbols + continuous lines) or screened wastewater (open symbols + dotted lines) recorded at the top measuring position. (top right pane) 18 mg/mL AgNP in screened wastewater dosed to 30 mg/L FeCl_3 recorded at the top measuring position (open symbols + dotted lines). The signal from *just* the wastewater, displaced by 3 cm^{-1} , is shown as a continuous line. (middle left pane) 37 mg/mL AgNP in nanopure water (open symbols + dotted line) and when dosed with 0.59 mg/L PSS (filled symbols + continuous lines) recorded at the top measuring position. (middle right pane) 37 mg/mL AgNP in nanopure water (open symbols + dotted line) and when dosed with 1091 mg/L PSS (filled symbols + continuous lines) recorded at the top measuring position. The inset shows the same data in log-log representation to highlight the similar Q -dependency of the scattering. (bottom left pane) 18 mg/mL AgNP in nanopure water (filled symbols) or screened wastewater (open symbols) recorded at the bottom measuring position. The dotted lines on this graph are fits to the composite polydisperse spheres model (see text). (bottom right pane) 18 mg/mL AgNP in nanopure water (filled symbols) or screened wastewater (open symbols) recorded at the bottom measuring position. The dotted lines on this graph are fits to the fractal cluster model (see text).

likely to encounter before entering, and once inside, a wastewater treatment plant. The choice of AgNP was largely a pragmatic one; to minimise sulphide formation and dissolution effects, and thus attempt to decouple the redox chemistry from the colloid chemistry, we chose passivated AgNPs, but then a

stabilising moiety was necessary to successfully disperse the nanoparticles in water (particularly given the ten-fold difference in density). Of the three most widely available stabilisers – citrate, PVP, and poly(ethylene oxide) (PEO) – the non-ionic stabilisers, and PVP in particular, have been shown to

be more successful at promoting dispersion than charged stabilisers like citrate.⁴⁹ Also, whilst a charge-stabilized nanoparticle would be expected to aggregate in the presence of background electrolyte or a counter-charged flocculant, the expectation from a sterically-stabilized nanoparticle is much less obvious. Our selection of PVP-stabilised AgNPs for this work also allowed us to investigate the uniqueness of the central result from our earlier work with silica NPs stabilized by a short-chain PEO-based surfactant.³⁹

In order to mimic the processes occurring in primary wastewater treatment, our measurements have been performed following established methodology, employing settlement microcosms in the form of tall cuvettes containing fresh wastewater. Small-angle neutron scattering (SANS) data have then been collected near the top (ie, nearest to the point of AgNP dosing) and the bottom of the cuvettes, allowing us to monitor the change in the AgNP size and concentration as a function of both time and position in the water column. The details of this are described in the Experimental section at the end of this paper, and in the Supplementary Information. Additional laboratory bench-top batch-sampling studies have also been conducted in order to cross-validate the SANS experiments. Our results enable us to propose a possible *mechanism*, hitherto unexplored in environmental nanoscience, behind the heteroaggregation responsible for the removal of non-ionic coated nanoparticles.

Results

SANS measures the angular variation in the intensity, $I(Q)$, of neutrons scattered from a sample, the diffraction angle being 'encoded' in a vector, Q . The intensity is proportional to the size and number concentration of the NPs, the Q -dependence of the scattering is determined by the shape of the nanoparticles. The behaviour of the AgNPs in the different matrices can be qualitatively observed from the treated SANS data (Figure 1, top and middle panes). These data are shown after subtraction of an essentially Q -independent background arising from the respective matrices (see point i below). From these data we can make the following observations:

- i. There is no appreciable signal from the wastewater alone (top-right panel, continuous line), nor from pure water (not shown), the former demonstrating that suspended solids in the wastewater do not produce an interference signal (they are either too dilute, too low contrast, or outside the measurement range of the instrument);
- ii. The dispersion stability of the AgNP in pure water on timescales exceeding 1.5 hours (top-left panel, filled symbols) is very high, the small loss in intensity with time indicating few NPs have settled out;
- iii. By contrast, the AgNP are very *unstable* in wastewater (top-left panel, unfilled symbols) with a two-thirds reduction in intensity in as little as 12 minutes, and approaching a 90% reduction in intensity after 2 hours;
- iv. Adding ferric chloride to the wastewater appears to promote some additional instability of the AgNP (top-right pane) – though these data were measured after longer times – but it has no effect on the wastewater itself on the timescale of the experiments (Figure S8);
- v. Adding PSS to the AgNP in pure water also promotes instability that progresses with time and which is more pronounced at higher PSS concentrations (middle-panes);
- vi. As there is no appreciable change in the Q -dependence of the scattering there does not appear to be any change in the shape of the AgNP in pure water, without and with,

added PSS (top-left pane and middle-panes). The same may also be true of the nanoparticles in wastewater but the poorer signal-to-noise in these data makes it difficult to be certain without a quantitative analysis.

The data presented in the top and middle panes of Figure 1 were all measured at the top of the sample cuvettes. The SANS data from near the bottom of the cuvettes are analogous, but for any given time have slightly higher intensity (bottom panes). This implies that the AgNP have settled.

To put these observations on a quantitative footing we have least-squares fitted the SANS data to analytical functions describing the shape and organisation of the nanoparticles in the different matrices (see Experimental). Example fits are shown in the bottom-panes of Figure 1 to a polydisperse spheres function (Equations 2 and 3) and a fractal cluster function (Equations 2, 3 and 4). For each matrix-time-position measurement this procedure yielded an apparent particle size and particle volume fraction (and cluster fractal dimension, where appropriate). The apparent volume fraction was then corrected by rescaling it against the known volume fraction of particles in a reference sample measured under similar conditions (see Supplementary Information). Across all the measurements performed there is an excellent correlation between the particle sizes and volume fractions derived from the two different functions, though the fractal cluster model tended to return slightly larger primary particle sizes and slightly smaller apparent volume fractions (See Figure S7).

With knowledge of the final particle volume fractions, Equation 5 could then be used to determine the mass concentration of AgNPs as a function of time in each of the different matrices. These are shown in the top-panes of Figure 2. Filled symbols correspond to the top of the cuvette, and open symbols the bottom. As inferred earlier, at a given time in a given matrix, the AgNP concentration is slightly higher nearer the bottom of the cuvette. In all instances the AgNP concentration decreases non-linearly with time, with the greatest change occurring in the first 30 minutes. Some of this change will be due to the differential settling velocities of different-sized NPs (see the PSD in Figure S1). These data can be adequately described by power law decays[†], the characteristic parameters for which are given in Table 1, and clearly illustrate a wide variation in dispersion stability between the different matrices. The principal source of uncertainty in these data is the uncertainty associated with the volume fraction, $\phi_{particles}$. This is very difficult to estimate. However as a guide, using the model-fitting parameters returned for the AgNP in water system (the most stable), the value of $\sigma / \langle \phi_{particles} \rangle \sim 7\%$, where σ is one standard deviation. It is reasonable to assume that this figure will be slightly higher in the systems exhibiting less stability (where the signal-to-noise was poorer), but even if doubled to 15% the differences between the concentration-time datasets for different media are still statistically significant.

From a wastewater treatment industry perspective a more insightful parameter is the settling velocity of the particles, v_s . Efficient primary clarification typically requires $\sim 100 < v_s < \sim 1000$ mm hr⁻¹ depending on the range of particle sizes in the influent^{S1,S2}, with the residence (hydraulic retention) time of the wastewater in the settling tanks typically engineered to be ~ 1 hour to a few hours, depending on influent load. We are able to calculate experimental settling velocities for the AgNPs from our data using the change in AgNP concentration relative to the known dosing concentration using Equation 6. The results are shown in the bottom-panes of Figure 2.

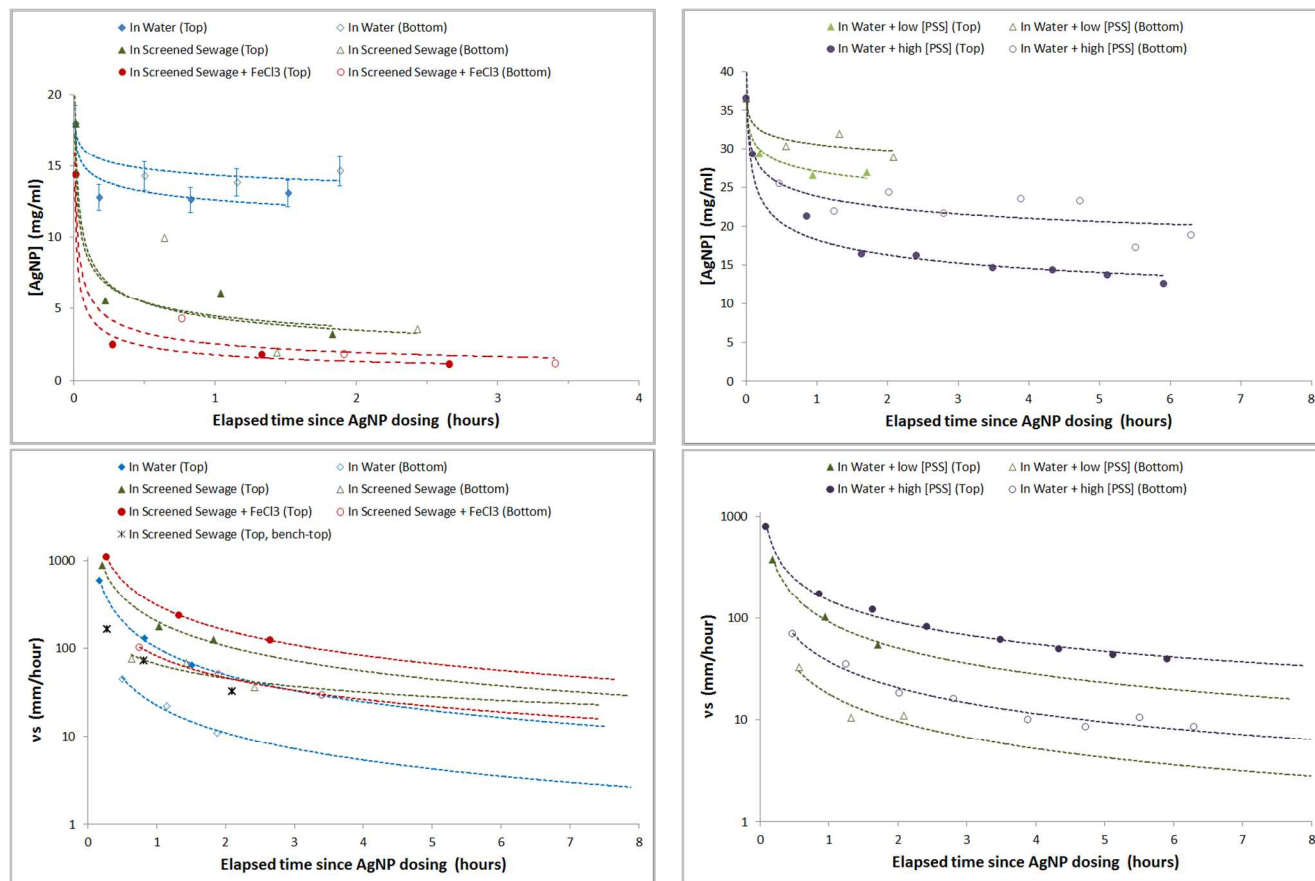


Figure 2: Time dependence of: (top left pane) AgNP concentration in nanopure water, screened wastewater, and screened wastewater dosed to 30 mg/L FeCl₃ recorded at the top (filled symbols) and bottom (open symbols) measuring positions. (top right pane) AgNP concentration in nanopure water dosed to 0.59 mg/L and 1091 mg/L PSS recorded at the top (filled symbols) and bottom (open symbols) measuring positions. (bottom left pane) AgNP settling velocity in nanopure water, screened wastewater, and screened wastewater dosed to 30 mg/L FeCl₃. Also shown are the settling velocities derived from the bench-top settling studies performed at much lower AgNP concentrations (see text). (bottom right pane) AgNP settling velocity in in nanopure water dosed to 0.59 mg/L and 1091 mg/L PSS. The dotted lines in all four graphs are power law trendlines to guide the eye. Error bars shown represent one standard deviation (see text).

Sample Matrix	Measuring Position	Average <i>D</i>	Average <i>R</i> (nm)	Loss (%)	[AgNP] trendline			<i>v_s</i> trendline		
					<i>A</i>	<i>n</i>	<i>R</i> ²	<i>B</i>	<i>m</i>	<i>R</i> ²
Water	Top	2.55 ± 0.03	10.4 ± 6.2	27	12.586	-0.066	0.816	101.620	-1.016	0.999
	Bottom	2.54 ± 0.02	10.3 ± 6.2	20	14.330	-0.046	0.896	22.757	-1.044	0.980
Screened Sewage	Top	3.38 ± 0.8	13.6 ± 8.2	74	4.480	-0.280	0.888	203.630	-0.941	0.992
	Bottom	3.38 ± 0.8	12.9 ± 7.7	78	4.338	-0.318	0.684	66.346	-0.528	0.775
Screened Sewage + FeCl ₃	Top	2.91 ± 0.4	7.6 ± 4.6	87	1.779	-0.423	0.980	311.470	-0.955	1.000
	Bottom	3.26 ± 0.7	10.9 ± 6.5	84	2.534	-0.384	0.924	82.012	-0.815	0.998
Water + low [PSS]	Top	2.58 ± 0.01	9.5 ± 5.7	25	27.043	-0.061	0.972	91.442	-0.853	0.996
	Bottom	2.58 ± 0.01	9.5 ± 7.7	16	30.555	-0.037	0.851	17.869	-0.895	0.853
Water + high [PSS]	Top	2.58 ± 0.01	9.7 ± 5.8	54	18.267	-0.163	0.964	149.660	-0.719	0.995
	Bottom	2.59 ± 0.01	9.8 ± 5.9	35	23.835	-0.091	0.807	37.304	-0.851	0.970

Table 1: Parameters describing the fractal floc structure (Eqn. 4), degree of AgNP removal at 1 hour, and simple power law trendlines $[AgNP] = A \times t^n$ and $v_s = B \times t^m$ in Fig. 2, where t is the elapsed time in hours and R^2 is a statistical measure of the goodness-of-fit. Note: the trendlines are unreliable at $t < 30$ seconds.

For comparison, the much larger TweenTM-capped SiO₂NPs in our previous work were determined to have a settling velocity $v_s \sim 80 \text{ mm hr}^{-1}$,³⁹ but these were of course much less dense. By contrast, the Stokes settling velocity of the AgNP in pure water

calculated from Equation 7 (for radius, $R = 10 \text{ nm}$) is just $v_{s, \text{stokes}} \sim 6.7 \times 10^{-3} \text{ mm hr}^{-1}$ (equivalent to 1.8 nm s^{-1} , or about $20 \mu\text{m}$ in a 3 hr SANS experiment).[§]

In all matrices, but particularly in wastewater, the derived v_s exceeds 100 mm hr^{-1} during the first hour at the top measuring position (equivalent to where influent wastewater would enter the settling tank). The corresponding efficiency of AgNP removal is shown in Table 1, as calculated from the trendlines shown in the bottom panes of Figure 2 at $t = 1 \text{ hr}$. It can be seen from Table 1 that the wastewater is almost *three times* more effective at removing the AgNP as pure water alone, and almost *twice* as effective as pure water with the high dose of PSS. The low dose of PSS essentially had no effect. Adding ferric chloride to the wastewater enhances AgNP removal by around 10% compared to the wastewater alone.

To cross-validate the results from the SANS experiments we have also performed a bench-top settling experiment using real wastewater. In order that the AgNP concentrations could be determined by ICPMS we used a much lower, and more environmentally-relevant, particle concentration (\sim hundreds of $\mu\text{g/L}$). Nevertheless, the results (see Table S6) directly correspond with those from the SANS experiments: after 2 hours just over 60% of AgNPs were removed from the top of the water column. The derived settling velocities – which actually represent a vertical positional average over some 60 mm as compared to just 8 mm in the SANS experiments – are plotted in the bottom-left pane of Figure 2 (star symbols) and lie between the trendlines from the SANS experiments in wastewater.

In the SANS experiments we deliberately did not measure the scattering at the very bottom of the cuvette, but the design of our bench-top experiment made it relatively straightforward to extract and analyse this fraction of the water column. As one would anticipate, we find particles removed from the top of the water column accumulate at the bottom.

Whilst our settling velocities may not be directly transferrable to a WWTP where there will be other mitigating factors, they should certainly be indicative, and are most definitely internally self-consistent.

Discussion

At this point we remind the reader that the only parameter that this study has in common with our earlier work is that the adsorbed stabiliser is *non-ionic*; the particle interfaces are chemically distinct with different degrees of surface ionisation (where exposed) and curvature, the chemical structure and molecular weight (ie, length) of the stabilisers are different, and the wastewater was sourced from different WWTPs at different times. Yet it is clear that something in the wastewater is as effective at colloiddally destabilising the PVP-capped AgNPs in this study as it was the TweenTM-capped SiO₂NPs in our earlier work. We have previously ruled out the background ionic strength of wastewater ($<0.01\text{M NaCl}$ equivalent) as an explanation for the rapid settlement of the NPs³⁹ and discuss this further later on. Another important result from our earlier work was that *uncapped* SiO₂NPs did not settle (in wastewater or pure water).

Mechanism of NP removal. The most logical explanation for our findings, therefore, is that there are specific interactions between the PVP or TweenTM coatings and some component(s) of the wastewater. In this respect it is interesting to note that the fractal dimension of the AgNP ‘flocs’ in Table 1 appear to jump from ~ 2.5 in pure water to just over 3 in wastewater (though the poor signal-to-noise of the latter data gives rise to large uncertainties) with only a small variation in primary particle size. This change in fractal dimension could be

consistent with a change from AgNPs with ‘normal’ PVP coatings to AgNPs with ‘entangled’ PVP coatings, or perhaps even the formation of a weak network entrapping the nanoparticles; but there is clearly no significant particle clustering taking place, else the SANS analysis would detect it. There are three pieces of evidence that shed some light on a possible mechanism behind our findings: first, the fact that at the pH of wastewater the *uncapped* SiO₂NPs from our previous work would have had *negatively-charged* interfaces; second, the stability of those NPs in wastewater; and third, the stability of Hou *et al*’s⁴⁸ citrate-capped AgNPs (ie, NPs that also had an interface with a dense population of close-bound negative charges) in wastewater. For these negatively-charged NPs to be electrostatically stabilized (citrate is too short to be an effective steric barrier) implies that they are not interacting with positively-charged components in wastewater and that, in turn, to explain the instability of the *capped* NPs our attention should be directed to those uncharged or negatively-charged components present. Here, the ability of a sufficiently high concentration of *anionic* PSS to destabilise the PVP-capped AgNPs (Figure 1, middle panes) suggests that it is in fact negatively-charged components that may be the key.

Limbach *et al*⁴⁰ have implicated peptones – mixtures of polypeptides and amino acids derived from partially-hydrolysed proteins – in the stabilisation of *uncapped* ceria NPs. We also note that the isoelectric points of all but two amino acids are *less* than the pH of our wastewater, and so the net charge on amino acids and peptides would be negative in our experiments. Similarly there are many anionic polysaccharides, derived from the degradation of plant biomass that will find their way into wastewater. But why should anionic components of wastewater interact with the non-ionic coatings on our NPs?

A possible insight comes from the seemingly unrelated areas of detergency and fabric conditioning. These applications deliberately exploit synergistic interactions between mixtures of short-chain ionic and non-ionic surfactants, but this can also lead to *co-adsorption* of the different species at an interface. An excellent demonstration of this effect has been provided by Penfold *et al*⁵³, who showed that the anionic surfactant sodium dodecyl sulphate (SDS) could be made to adsorb on a negatively-charged silica surface in water in the presence of the non-ionic surfactant hexaethylene glycol monododecyl ether (C₁₂E₆), provided there was a molar excess of C₁₂E₆. In the absence of C₁₂E₆ there was no adsorption of the SDS, as one would expect. (The same authors also demonstrated similar behaviour with a cationic surfactant in place of the SDS at a different pH⁵⁴). The amount of SDS adsorbed was small, $<1 \text{ mole}\%$, even when the amount in solution was tens of mole%, and the adsorbed SDS was only located at the outer region of the mixed adsorbed layer, but it nonetheless indicates that anionic and non-ionic species can interact under specific conditions. Penfold *et al* ascribed the co-adsorption to favourable packing of the (hydrophobic) alkyl ‘tails’ *but also* to headgroup interactions, noting that in ionic/non-ionic surfactant mixtures the mixing process dilutes what would otherwise be unfavourable electrostatic interactions between the charged SDS headgroups. However, this also provides an environment in which those charged headgroups can then interact through van der Waals forces with weak dipoles in the headgroups of the uncharged surfactant molecules. We believe this is the mechanism that is ultimately responsible for the instability of our non-ionic surfactant-coated NPs in wastewater, particularly if the co-adsorbing species also interacts with other oppositely-

charged components (cationic polysaccharides, mineral particles, etc).

Though Penfold *et al* studied two surfactants adsorbing from bulk solution, it is not unreasonable to consider that a pre-adsorbed layer of non-ionic surfactant would constitute a local excess and so promote analogous behaviour. If so, one might also speculate that the same would apply to non-ionic surfactants interacting with a pre-adsorbed layer of ionic surfactant, such as in the systems studied by Limbach *et al*⁴⁰ and Wang *et al*⁴³.

Challenging our interpretation. But how robust is this interpretation? We shall now consider potential alternative explanations.

Particle concentration. The most serious criticism that can be levelled at this work is its use of an environmentally-unrepresentative concentration of AgNPs, raising the question of whether the particle concentration itself could in some way have influenced the outcome of the study. There is no evidence to support this concern, and indeed we present direct evidence that refutes it.

Whilst the *mass concentration* of AgNPs on dosing was high (18 mg/ml), because of the high density of silver the *volume fraction* of AgNPs was a mere 0.19% (ie, $\phi \sim 0.002$). This is important, because the thermodynamics of colloidal systems are expressed in terms of volume fraction⁵⁵ in much the same way that the colligative properties of a chemical system are normally expressed in terms of molality. A volume fraction of 0.19% is a *very low* value. Some measure of this may be gained from the impact of ϕ on the interparticle structure factor $S(Q)$, because if interparticle interactions between the AgNPs were important they would manifest themselves in the SANS through Equation 2. In Figure S9 we provide calculations of $S(Q)$ and $I(Q)$ for dispersions of spherical particles having the same physical characteristics as the AgNPs used in our study. The cases of both uncharged and charged particles are considered, but it is clear that at the particle volume fraction we have used interparticle interactions are negligible in both cases. Furthermore, in our earlier work³⁹ with (larger) SiO₂NPs we used a lower volume fraction of 0.10% (an equivalent mass concentration of 2.5 mg/ml for that system) yet observed completely analogous behaviour to that described in the present study. But the final, perhaps most compelling, piece of supporting evidence, are the results from our bench-top settling experiment. Performed at a very much lower particle concentration, they demonstrate the same behaviour of the AgNPs, to broadly similar extents, over the same timescales, as found from the SANS experiments (Figure 2, bottom-left pane).

Homo- vs hetero-aggregation. One reason why high AgNP concentrations could be an issue is that it might promote homo-aggregation of the AgNPs. In contrast, primary clarification is a predominantly hetero-aggregation process. So might we have studied a different process? As we have outlined above, NP-NP interactions are negligible at the particle volume fraction we have used (and $S(Q)$ depends explicitly on the interaction potential). But in any event, homo-aggregation between 'like' particles is inherently a kinetically unfavourable process (one reason why water treatment companies use flocculating agents) and so is unlikely to explain the rapid particle removal we see in our study. And the same concentration of the same AgNPs but dispersed in pure water is ostensibly stable on the same timescales as when it is dispersed in wastewater (Figure 1, top-left pane). If our particle concentration was so high as to be driving homo-aggregation it would surely do so in both pure water and wastewater. Instead, our results quite clearly show that at least one other component is necessary to induce aggregation. The mechanism for particle removal we have put forward is a hetero-aggregation process that does not require NP-NP interactions.

The absence of homo-aggregation between our AgNPs is also supported by the results of the SANS data model-fitting. First, there is no systematic increase in the derived particle size with time (Figure S10), as would be expected if the AgNPs were aggregating into clusters. Second, the fractal dimensions for the floc structures we report in Table 1 are not what would be expected for aggregate structures formed through either diffusion-limited ($D \sim 1.8$) or reaction-limited ($D \sim 2.1$) particle cluster mechanisms. And the absence of homo-aggregation is further strengthened by the similarity of the results from the bench-top settling experiments performed at much lower AgNP concentration.

Particle transformation. As discussed in the Introduction, AgNPs are subject to chemical and physical transformation in the environment. The extent of any transformation will therefore have an impact on how the AgNPs interact with dissolved and suspended components in the wastewater. Just as Figure S10 shows that there is no increase in particle size on the timescales of our experiments, *neither does it show any clear decrease in particle size*. From this we can conclude that there was no significant dissolution of our AgNPs. However, this is perhaps not too surprising. Our AgNPs have a thin oxide layer and Ag₂O is only poorly soluble in water. And the principle environmental transformation pathway for elemental silver is via sulphidation and Ag-S species exhibit similarly poor solubility in water. Indeed, as Levard *et al*³⁴ show, sulphidation retards the dissolution of AgNPs. The conditions for sulphidation are also more prevalent in more anaerobic environments, such as in sludge, than they are in wastewater as used in our studies. Third, there is the issue of the timescales for particle transformation. This appears to depend on both the duration of exposure of AgNPs to an oxidising environment and on the size of the AgNPs. At around \sim pH 7 - 8: Liu *et al*³⁰ report <10% dissolution of 20 nm citrate-capped AgNPs after 3 hours in a biological media; Kaegi *et al*³⁵ report \sim 15% sulphidation of PVP-coated AgNPs after 5 hours in wastewater, complete sulphidation of 10 nm citrate-capped AgNPs in sludge after 24 hours, but only 10% sulphidation of 100 nm citrate-capped AgNPs in sludge after the same period; and Impellitteri *et al*⁴⁶ also report complete sulphidation of citrate-capped AgNPs in sludge within 24 hours, though the particle size is unclear. Thus on the timescales of primary wastewater treatment, and our experiments, say 1 - 3 hours, but <6 hours at most, the degree of transformation of our \sim 10 - 40 nm PVP-coated AgNPs may be no more than 10%. Implicit in this discussion is the assumption that formulated coatings on engineered NPs will also be gradually degraded, maybe even exchanged, during transit of the NPs through the wastewater system and treatment process. The duration of exposure and exact conditions will again be the controlling factors, with short exposure to wastewater (as in our experiments) being a less severe treatment than prolonged incubation in sludge⁵⁶.

Other interaction mechanisms. A recognised mechanism for destabilising naturally-occurring colloids in environmental matrices is that of 'calcium bridging', whereby Ca²⁺ (but potentially other multivalent cations) electrostatically complex with anionic components, leading to aggregation and sedimentation. The anionic components may, of course, differ and either be surface-adsorbed, or in solution, or indeed, both, and there is evidence that the latter does actually lead to enhanced sedimentation. The problem with attempting to use this electrostatic mechanism as an explanation for our results is that it is ineffectual when the NPs are coated with a non-ionic steric stabiliser (such as PVP), even in the presence of dissolved NOM.⁵⁷ Thus, the only way our AgNPs could be directly destabilised by cation bridging would be if the PVP coating was incomplete *and* the exposed NP surface had a negative charge. However, whilst some degradation of the coating is likely, as

discussed above, at the pH of wastewater Ag_2O is positively-charged (the PZC is $\sim 10.1 - 11.2$).^{58,59}

In situations where the NPs have patchy steric coatings it is sometimes possible to get interparticle bridging by the stabiliser. However this requires the NPs to be able to approach within each other's sphere of influence, often enough, and, in the case of NPs with charged surfaces, compression of the surrounding electrical double layers (else the NPs will repel one another). In our earlier work³⁹ we demonstrated that *uncoated* SiO_2 NPs did not settle in wastewater, indicating that the ionic composition and ionic strength of wastewater was not sufficient to coagulate those (negatively) charge-stabilised NPs through compression of their double layers. We then performed a series of coagulation studies on the non-ionic surfactant-coated SiO_2 NPs using $\text{La}(\text{NO}_3)_3$; ie, a cation an order of magnitude more effective at coagulating charged particles than Ca^{2+} (Schultze-Hardy rule). The results showed that only when the ionic strength of the medium was much *higher* than that of the wastewater could we even begin to coagulate the coated SiO_2 NPs on anything like the same timescale as the wastewater alone was achieving. This observation is indirectly reinforced by our present data where we added FeCl_3 to the wastewater – there is only a small enhancement in AgNP removal over what wastewater alone achieved. Also reinforcing our observations in this regard are the stability of Hou *et al*'s citrate-capped AgNPs in wastewater⁴⁸, and the very recent work of Zhou *et al* with uncapped ZnO and TiO_2 NPs⁶⁰. The ionic strength of wastewater is approximately equivalent to $\sim 0.01\text{M}$ NaCl, for which the double layer thickness would be of the order of 2 nm. This happens to be about the same as the radius-of-gyration of the PVP-coating on our AgNPs; ie, the AgNPs would need to approach very close to one another indeed.

A related mechanism would be interparticle bridging by other components in wastewater. But again, the same physical constraints in respect of stabiliser coverage, double layer thickness and NP encounter frequency discussed above, would still apply. The most likely agents for such bridging would be humic/fulvic acids and similar charged 'polymer-like' species, but in the case of our AgNPs only anionic species could adsorb to the Ag_2O surface (and an equivalent mechanism, but with *cationic* components in wastewater, would need to have occurred in our SiO_2 NP work). Though it is tempting to identify the effect of added PSS on our AgNPs (Figure 1, middle-panels) as proof of this mechanism there are in fact significant issues. First, our PSS data were measured in water, not wastewater, and so one would not expect (any) significant loss of the PVP stabiliser (or other transformation of the NPs) to facilitate the bridging. Second, the rate of settling in the AgNP-PSS-water systems is a lot slower, and particle removal is less efficient, than in the AgNP-wastewater systems, even though the Rg of the PSS flocculant is approximately six times that of the PVP. Taking all these factors together, it seems unlikely that destabilisation of our AgNPs by interparticle bridging as a result of incomplete PVP coatings could be a significant mechanism, at least on the timescales of primary clarification.

In the last couple of decades mainstream colloid science has recognised the importance of what has become known as the hydrophobic interaction, an entropy-driven effect where the association of hydrophobic moieties disrupts the usual cage-like structure formed by hydrogen-bonding water molecules. The effect is now implicated in processes such as the folding of proteins, for example. The strongest hydrophobic interactions occur at elevated temperatures, in systems of long linear aliphatic organic molecules, but Song *et al*⁶¹ have provided evidence that the hydrophobic interaction is likely responsible for the attachment of non-ionic (including PVP) coated AgNPs to C_{18} chemically-hydrophobised glass beads. However,

attachment efficiencies did not exceed 16% even under the most favourable coverage conditions with a PVP stabiliser 67% longer ($M_w \sim 10000$ g/mol) than that on our AgNPs. Thus, whilst we cannot rule out hydrophobic interactions in the systems we have studied, it seems unlikely that they could be the dominant mechanism responsible for NP removal. More problematic in any case is the fact that, in wastewater, any truly hydrophobic substances (mimicking the hydrophobised glass beads), such as fat particles and oil droplets, will be solubilised. Substances like fatty acids, of course, meet our description of 'anionic components'. There is some literature on the adsorption of alkanes into non-ionic surfactant layers at the macroscopic oil-water interface⁶², but this showed adsorption to increase with activity; ie, the adsorption of short alkanes was favoured. This process would not therefore produce a hydrophobic interaction strong enough to drive aggregation.

Environmental perspective. One final observation that we may make is that the *total* naturally-occurring NP background in our wastewater sample must be considerably less than the minimum AgNP concentration we derive, 1.2 mg/ml (Figure 2, top-left pane), otherwise the SANS from the wastewater alone (Figure 1, top-right pane) would not be a flat line. This upper bound on the NP concentration is consistent with the recent analytical work of Johnson *et al*⁵⁰ that measured the average concentration of 'colloidal' silver (defined as being in the size range 2 – 450 nm) in a range of UK wastewaters at a very low $\sim 10^{-8}$ mg/ml. This concentration of AgNPs is well below levels that have been shown to be toxic to microbes present in biofilms in secondary wastewater treatment. For example, Amaout²⁶ has shown that nitrite production by *N. europaea* can be inhibited by as much as 15% at AgNP concentrations of 0.002 – 0.02 mg/ml, depending on the surface coating (citrate and gum Arabic both inhibiting more effectively than PVP). At even higher AgNP concentrations cell lysis was observed. Within mixed microbial communities some individual communities were initially affected by the addition of AgNPs more than others, but overall there was greater resilience, perhaps evidence of adaptation to the change in chemical environment. These findings appear to be borne out by Giska.²⁷ Sheng *et al*²⁴ observed that whilst isolated cultures could be wiped out by 0.001 mg/ml of AgNP (*Thiotrichales* was particularly susceptible), mixed biofilms were still resilient at 0.2 mg/ml. And Doolette *et al*⁴⁷ have noted that whilst transformed (into Ag-S species) AgNPs "did not affect the dominant populations of nitrifiers and methogenic organisms in aerobic and anaerobic generated sludges... a subtle shift in niche populations was observed" (the latter being more evident in anaerobically-digested sludges).

Together, these studies, and the findings we report here, would seem to indicate that AgNPs entering WWTPs in raw sewage pose no significant risk to secondary treatment biofilms at the present time. Where there may be greater cause for concern, however, is in the post-treatment disposal of the sewage sludge. This is because the sewage sludge is effectively a sink for the AgNPs and the practice of adding it to land as an agricultural fertiliser means that there is the potential for AgNPs, or their oxidation products (eg, Ag_2S), to accumulate in the soil. As Johnson *et al*⁵⁰ have noted, this aspect of the lifecycle of AgNPs is not yet well researched, though Whitley *et al*⁵⁶ have recently pointed to the profound impact that the presence or absence of the surface coating can have on the partitioning of NPs to soil pore water.

Experimental

Materials.

Nanoparticles and chemicals. Partially-passivated silver nanopowder of median diameter 22 nm was sourced from American Elements (Product code AG-M-025M-NPC.030N; Merelex Corporation, California, USA). This particular product came coated with a poly(vinylpyrrolidone), PVP, stabiliser ($M_w \sim 6000$ g/mol) to enhance its dispersion in water. Poly(sodium 4-styrenesulphonate), PSS, flocculant (average $M_w \sim 70000$ g/mol) was sourced from Sigma-Aldrich (Gillingham, Dorset, UK). Iron (III) chloride hexahydrate flocculant was sourced from Merck Millipore (Watford, Hertfordshire, UK). Nanopure water (18 M Ω resistivity) was produced in-house (Barnstead International Diamond system).

Wastewater. Raw (untreated) wastewater was sourced from the inlet stream of a wastewater treatment plant in Oxfordshire, UK serving a rural population of just over 6000 people. Prior to use the wastewater was 'screened' by passage under gravity through a glass wool plug (for the SANS measurements) or fine sieve (for the bench-top measurements) in order to remove floating debris and fibrous material on mm length scales.

Small-angle neutron scattering (SANS).

Instrumentation. SANS measurements were conducted on the *LOQ* diffractometer at the ISIS Facility (STFC Rutherford Appleton Laboratory, Oxfordshire, UK).⁶³ This is a fixed-geometry polychromatic instrument which utilises neutron wavelengths λ between 2.2–10 Å to simultaneously probe scattering vectors Q between 0.008–1.6 Å⁻¹ (equivalent d-spacings of 0.4–78 nm) where

$$Q = (4\pi \sin(\theta)) / \lambda \quad (1)$$

and 2θ is the scattering angle. To comply with biological safety protocols, the samples to be measured were contained in custom-made 100 (h) x 20 (w) mm fused silica screw cap cuvettes of 2 mm pathlength (Optiglass Ltd, Essex, UK), pairs of which were housed inside custom-built, hermetically-sealed, containment vessels with neutron-transparent windows.³⁹ The containment vessels were mounted on top of a computer-controlled horizontal translation stage, itself sat on top of a computer-controlled vertical height stage. It was thus possible to scan the height of either cuvette by remote control. The neutron beam was collimated to a rectangular slit 8 (h) x 15 (w) mm immediately before the containment vessel beam entry window. To monitor particle settling, SANS data were recorded at two vertical positions: one 9 mm above ('bottom'), and the other – because adding flocculants changed the height of the meniscus – 64 or 72 mm above ('top'), the base of the cuvettes (these distances refer to the centre of the beam aperture). Background SANS (on nanopure water and screened wastewater) and neutron transmission measurements were performed 57 mm ('middle') above the base of the cuvettes. SANS data were collected on each sample in approximately 20–30 minute intervals over periods of 2–7 hours. Measurements were performed at ambient temperature (circa 21°C on May 5-7 2010, and circa 23°C on May 28-29 2010).

Sample preparation. A 16.5 %_w stock dispersion of the nanoparticles was prepared by directly adding the nanopowder to nanopure water and then sonicating (Fisherbrand FB11021, Fisher Scientific, UK) for 5 minutes at ambient temperature. This procedure yielded a homogeneous dispersion (see Figure S3). After brief manual re-agitation, 400 μ L of the stock

dispersion was then added to 3.2 mL of nanopure water or wastewater, thereby yielding a maximum initial particle concentration on dosing of 0.19 %_v; equivalent to a mass concentration of 18 mg/ml. This dosing concentration was chosen on the basis of our previous experience with similar systems,^{39,64} and the need to produce a statistically significant SANS signal in a measurement time frame typical of particle settling in primary treatment tanks; it was not intended to be representative of actual environmental concentrations, nor to be so high as to invoke interparticle interactions (see Figure S9). Further mixing was achieved by simply inverting the cuvettes several times. This mixing was repeated immediately before data collection was initiated because of the inevitable delays in loading and resealing the containment vessel and then transporting it to the *LOQ* diffractometer (~1 hr). For the experiments with added flocculant, an *additional*: (i) 160 μ L of 630 mg/L FeCl₃ solution (to give 30 mg/L in the cuvette), (ii) 200 μ L of 10 mg/L PSS solution ('low [PSS]', to give 0.58 mg/L in the cuvette), or (iii) 200 μ L of 18550 mg/L PSS solution ('high [PSS]', to give 1091 mg/L in the cuvette) were added to nanoparticle dispersions in wastewater or nanopure water. These flocculant concentrations were chosen to be representative of those used in the wastewater treatment industry.^{65,66,67,68,69}

Data treatment. Raw scattering data were corrected for the experimentally-determined neutron transmission and background scattering of each sample, the sample pathlength, and for the efficiency and spatial linearity of the detectors, according to standard procedures using the instrument-specific software *COLETTE*,⁷⁰ before being converted into scattered neutron intensity data, $I(Q)$. These treated ('reduced') data were then placed on an absolute intensity scale by comparison with the scattering from a well-characterised polymer calibration standard measured with the same instrument configuration.⁷¹

Data analysis. The SANS per unit volume from a two-component sample may be written in a very general form as

$$I(Q) = K \phi_1 \phi_2 (\rho_1 - \rho_2)^2 P(Q) S(Q) + B \quad (2)$$

where K is a calibration factor, and ϕ_i and ρ_i are the volume fraction ($\phi_1 + \phi_2 = 1$) and neutron scattering length density of component i , respectively. The term in brackets – known as the 'contrast' – quantifies the visibility of component 1, whilst $P(Q)$ – the 'scattering law' – describes how the scattering is modulated by particle size and shape. $S(Q)$ – the 'structure factor' – describes how the scattering is modulated by interparticle interactions. B is the residual background signal. Parameters such as the particle size and particle volume fraction were derived from the $I(Q)$ data, assuming $\rho_{\text{particles}} = +2.81 \times 10^{10}$ cm⁻² and $\rho_{\text{H}_2\text{O}} = -0.56 \times 10^{10}$ cm⁻², by least-squares model-fitting a function for $P(Q)$, integrated over a wide range of particle radii, R (here $\sigma / \langle R \rangle \sim 0.6$ (60%), if σ is the standard deviation of the size distribution), using the program *SasView*.⁷² In the case of a sphere

$$P(Q) = \left[\frac{3(\sin(QR) - QR \cos(QR))}{(QR)^3} \right]^2 \quad (3)$$

At the particle concentrations used in this work we found it unnecessary to invoke specific interparticle interaction potentials during the data fitting; ie, it was assumed that $S(Q) = 1$. In earlier work^{64,73} we have also shown that these sorts of system can sometimes be described in terms of fractal

cluster models where Eq 3 is used to describe the spherical 'building blocks' of the cluster and⁷⁴

$$S(Q) = 1 + \frac{D \Gamma(D-1) \sin[(D-1) \tan^{-1}(Q\xi)]}{[1+1/(Q\xi)^2]^{(D-1)/2} (QR)^D} \quad (4)$$

Here D is the fractal dimension and ξ is related to the overall size of the cluster. Unfortunately these two quantities are correlated and so to facilitate the fitting we chose to fix the latter at $\xi = 73$ nm (ie, $> 5R$), the maximum length scale accessible on the LOQ diffractometer. Density correlations at this distance are expected to be negligible.⁷⁵

Calculation of settling velocities. Given an apparent volume fraction of nanoparticles $\phi_{particles}$ derived from analysis of the SANS data, the mass concentration of nanoparticles is then

$$c \text{ (mg/ml)} = \left[\frac{\delta_{AgNP} \times (100 \phi_{particles})}{(99 - (100 \phi_{particles}))} \right] \times 1000 \quad (5)$$

where δ_{AgNP} is the bulk density of the nanoparticles (9.49 g cm^{-3}). On the basis that a 100% change in the nanoparticle concentration over 100 mm in 1 hour constitutes an experimental settling velocity $v_{s,expt}$ of 100 mm hr^{-1} , one may then write

$$v_{s,expt} \text{ (mm/hr)} = \Delta c \times (100/d) \times (1/t) \quad (6)$$

where Δc is the percentage change in concentration, d is the distance below the meniscus (100 mm above the base of the cuvettes) in mm, and t is the elapsed time since mixing in hours.

By contrast, the Stokes settling velocity $v_{s,stokes}$ of a nanoparticle of radius R nm is⁷⁶

$$v_{s,stokes} \text{ (mm/hr)} = 3.6 \times 10^{-12} \left[\frac{2}{9} \frac{g}{\eta} (\delta_{AgNP} - \delta_{H_2O}) R^2 \right] \quad (7)$$

where the acceleration due to gravity $g = 980.67 \text{ cm s}^{-2}$ and the density and viscosity of water at $25 \text{ }^\circ\text{C}$ are $\delta_{H_2O} = 0.997 \text{ g cm}^{-3}$ and $\eta = 0.01 \text{ g cm}^{-1} \text{ s}^{-1}$, respectively.

Bench-top settling studies.

Experimental arrangement. As for the SANS experiments, a stock dispersion of the nanoparticles, but this time much less concentrated, was prepared by directly adding the nanopowder to nanopure water and then sonicating it for at least 5 minutes at ambient temperature. After brief manual re-agitation, 1 mL of this stock dispersion was dosed into 99 mL of wastewater in a 100 mL glass burette to give a dosed concentration of $<1000 \text{ } \mu\text{g/L}$; ie, a Ag concentration more representative of that entering WWTPs.⁵⁰ In addition, the available sedimentation depth in each burette was over 660 mm; ie, more than six times that in the SANS cuvettes, and closer to the depth of a typical primary sedimentation vessel (typically 1-2 m).

After some mixing, achieved by simply inverting the burette, a 10 mL ($t=0$ min) sample was immediately extracted from the top of the burette by syringe. After a given time, a further 10 mL sample was extracted from the top of the burette, and then a 10 mL sample was drawn off from the bottom of the burette through the tap. Samples were recovered in this way after 15, 45 and 120 minutes using a separate burette for each time point. Each sample was immediately stabilised by the addition of ultrapure nitric acid (Ultrex analytical grade, JT Baker, UK) before subsequent digestion in aqua

regia on a hotplate. This method is based on US EPA Method 200.2 and achieves good recoveries. Samples after digestion were optically transparent confirming the suitability of the method.

Instrumentation. The digests were typically diluted by a factor of ten with 1M hydrochloric acid (to ensure an excess of Cl⁻) and then measured using a Perkin Elmer Nexion 300D inductively coupled plasma mass spectrometer (ICPMS). Both Ag stable isotopes (¹⁰⁷Ag and ¹⁰⁹Ag) were measured, with the concentration data for ¹⁰⁷Ag reported here. Corrections were made for Zr (oxide) spectral interferences. Using both isotopes allowed cross-validation of the concentration data obtained. For all measurements the difference in Ag concentration determined from each isotope was typically less than 5%. The ICPMS instrument was calibrated using Ag standards over the range 0–10 $\mu\text{g/L}$ in 1M hydrochloric acid matrix using ¹¹⁵In as an internal standard to compensate for matrix effects and possible drift in instrument sensitivity. The resulting ICPMS instrument detection limit was $\sim 0.1 \text{ } \mu\text{g/L}$. To check for contamination, blanks containing ultrapure acids were analyzed along with the digests and were found to have non-detectable Ag levels. An un-dosed sample of wastewater was also digested and found to have a background Ag concentration of $1.4 \text{ } \mu\text{g/L}$.

Additional experimental details may be found in the Supplementary Information.

Conclusions

This study builds on our earlier work, and demonstrates that the rapid settling of NPs coated with non-ionic stabilisers in wastewater is a generic heteroaggregation effect. On entering WWTPs such NPs will be efficiently removed to the sewage sludge at the primary treatment stage.

The origin of the effect is, we believe, a synergistic interaction between the hydrophilic part of the stabilising moiety and anionic components present in wastewater (eg, peptones, polysaccharides), possibly even leading to entrapment of the NPs in a diffuse 'polymer-like' network which then interacts more widely with other (oppositely charged) components to enhance the settling velocities. This interaction has previously been ignored in discussions of nanoparticle behaviour in environmental matrices such as wastewater.

However, as others have noted^{16,18}, the natural environment is a complex chemical reactor where NPs are potentially subject to many different biotic and abiotic transformations; NPs entering the environment with surface coatings may lose them (and *vice versa*), or indeed gain different or mixed coatings. Thus determining a mechanism that controls the fate of NPs in the environment does not in itself necessarily determine *which* NPs are subject to that control. This of course has profound implications for modelling NP transport, whether in wastewater treatment or throughout the wider environment.

Our work also demonstrates that, in contrast to the predictions of the Stokes equation, NP settling velocities in complex environmental matrices are in fact time-dependent (though the *change* in settling velocity with time eventually reaches a steady-state, see Figure S11). This is a known phenomenon, due in part to the size polydispersity of the NPs but also, and particularly for wastewater treatment, the presence of density stratifications in the settling tank.⁷⁷ The mechanism we have outlined, and thus the settling velocities derived, will also be dependent on the concentration of both the NPs and the wastewater components with which they interact.

Though real wastewater treatment is a much more dynamic environment than that we have modelled, WWTPs are normally

operated in such a way as to give primary clarification the greatest ability to succeed. Our results could potentially help plant operators adapt their procedures to enhance the removal of ENMs alongside the normal colloidal and mesoscale detritus.

Acknowledgements

We thank H. Al-Obaidi for taking the TEMs of the NPs; D. Myatt and L. Clifton for making the DLS measurements; S. Waller and B. Holsman for the design of the Biological Containment Vessels; the ISIS Facility for funding construction of the vessels and providing neutron beam time (Experiment RB1010250); and Thames Water Utilities Limited for granting access to the treatment works. The work described was funded by the UK Science & Technology Facilities Council, the UK Natural Environment Research Council, and by the EU Framework Programme 7 *NanoFATE* project. The data analysis benefitted from use of the *SasView* software originally developed by the *DANSE* project under US National Science Foundation award DMR-0520547. Finally we would like to thank the anonymous Referee's and the Editor. Their careful critique led us to re-examine several aspects of our presentation and as a result the revised manuscript has benefitted significantly.

Notes and references

^a *ISIS Facility, STFC Rutherford Appleton Laboratory, Harwell Oxford, Didcot, OX11 0QX, United Kingdom. E-mail: stephen.king@stfc.ac.uk. Tel: +44 (0)1235 446437.*

^b *NERC Centre for Ecology & Hydrology, Mclean Building, Benson Lane, Crowmarsh Gifford, Wallingford, OX10 8BB, United Kingdom.*

^c *NERC Centre for Ecology & Hydrology, Lancaster Environment Centre, Lancaster LA1 4AP, UK, United Kingdom.*

^d *Pharmaceutical Science Division, King's College London, Franklin-Wilkins Building, Stamford Street, London, SE1 9NH, United Kingdom.*

† Though logarithmic trendlines actually return slightly better statistical R^2 -factors than the power law trendlines shown when describing the concentration-time data, the long time behaviour of these functions is unphysical for some datasets (resulting in negative concentrations). Either type of trendline is however arbitrary.

§ It would take AgNPs settling at this velocity 50 days to transit the 8 mm high window illuminated by the neutron beam.

Electronic Supplementary Information (ESI) available: characterisation data for the silver nanopowder; TEMs of the silver nanopowder; estimation of the radius-of-gyration of the PVP stabiliser; schematic representation of a silver nanoparticle; neutron scattering length densities and contrasts; SANS characterisation data for the silver nanopowder dispersions; SANS model comparisons; characterisation data for the wastewater; results of the bench-top settling experiments; effect of FeCl_3 on the SANS from wastewater; impact of particle volume fraction on colloidal interactions; resilience to dissolution of the AgNPs; rate of change of the NP settling velocities; temperature history during the SANS experiments. See DOI: 10.1039/b000000x/

¹ 'Nanoscale Chemicals and Materials', SRI Consulting, December 2010; <http://www.ihs.com/products/chemical/planning/scup/nanoscale-chemicals.aspx> (accessed 29/07/2014).

² 'Global Nanomaterials Opportunity and Emerging Trends', Lucintel, March 2011; <http://www.lucintel.com/LucintelBrief/GlobalNanomaterialsoportunity-Final.pdf> (accessed 29/07/2014).

³ 'World Nanomaterials to 2016', Study # 2871, The Freedonia Group, Inc. May 2012; <http://www.freedoniagroup.com/World-Nanomaterials.html> (accessed 29/07/2014).

⁴ 'Types and uses of nanomaterials', European Commission Document 52012SC0288, October 2012; <http://eur-lex.europa.eu/legal-content/EN/TXT/PDF/?uri=CELEX:52012SC0288> (accessed 29/07/2014).

⁵ C. O. Hendren, X. Mesnard, J. Dröge, M.R. Wiesner, *Environ. Sci. Technol.* 2011, **45**, 2562.

⁶ F. Piccinno, F. Gottschalk, S. Seeger, B. Nowack, *J. Nanoparticle Res.*, 2012, **14**, 1109.

⁷ 'The Global Market for Metal Oxide Nanoparticles to 2020', Future Markets, Inc. March 2013; <http://www.reportsnreports.com/reports/236441-the-global-market-for-metal-oxide-nanoparticles-to-2020.html> (accessed 29/07/2014).

⁸ 'Roadmap Report on Nanoparticles', NanoRoadMap, November 2005; <http://nanoparticles.org/pdf/PerezBaxEscolano.pdf> (accessed 29/07/2014).

⁹ European Commission, Memo/12/732, October 2012; http://europa.eu/rapid/press-release_MEMO-12-732_en.htm (accessed 29/07/2014).

¹⁰ 'Nanosilver: Safety, Health and the Environmental Effects and Role of Antimicrobial Resistance', Silver Nanotechnology Working Group, The Silver Research Consortium, LLC, May 2012; <https://www.silverinstitute.org/site/wp-content/uploads/2013/05/SNWGSubmissiontoSCENIHR.pdf> (accessed 29/07/2014).

¹¹ N. Seltnerich, *Environ. Health Perspect.*, 2013, **121**, A220.

¹² 'Global Market for Nano Silver', Research and Markets, May 2012; http://www.researchandmarkets.com/reports/2124534/global_market_for_nano_silver.pdf (accessed 29/07/2014).

¹³ T. Benn, B. Cavanagh, K. Hristovski, J.D. Posner, P. Westerhoff, *J. Environ. Quality*, 2010, **39**, 1875.

¹⁴ F. Gottschalk, B. Nowack, *J. Environ. Monit.*, 2011, **13**, 1145. **Review.**

¹⁵ B. Nowack, T.D. Bucheli, *Environ. Pollut.*, 2007, **150**, 5. **Review.**

¹⁶ G.V. Lowry, E.M. Hotze, E.S. Bernhardt, D.D. Dionysiou, J.A. Pedersen, M.S. Wiesner, B. Xing, *J. Environ. Qual.*, 2010, **39**, 1867.

¹⁷ D. Lin, X. Tian, F. Wu, B. Xing, *J. Environ. Qual.*, 2010, **39**, 1896.

¹⁸ E.S. Bernhardt, B.P. Colman, M.F. Hochella, B.J. Cardinale, R.M. Nisbet, C.J. Richardson, L.Yin, *J. Environ. Qual.*, 2010, **39**, 1954.

¹⁹ A.B.A. Boxall, K. Tiede, Q. Chaudry, *Nanomedicine*, 2007, **2**, 919.

²⁰ V.L. Colvin, *Nat. Biotechnol.*, 2003, **21**, 1166.

²¹ M.R. Wiesner, G.V. Lowry, P. Alvarez, D. Dionysiou, P. Biswas, *Environ. Sci. Technol.*, 2006, **40**, 4336.

²² J. Evans, *Chem. World*, 2006, **3**, 58.

²³ N. Musee, M. Thwala, N. Nota, *J. Environ. Monit.*, 2011, **13**, 1164.

Review.

²⁴ Z. Sheng, Y. Liu, *Water Res.*, 2011, **45**, 6039.

²⁵ A. García, L. Delgado, J.A. Torà, E. Casals, E. González, V. Puentes, X. Font, J. Carrera, A. Sánchez, *J. Haz. Mater.*, 2012, **199–200**, 64.

²⁶ C.L. Arnaout, PhD Thesis, Duke University, 2012; http://dukespace.lib.duke.edu/dspace/bitstream/handle/10161/5852/Arnaout_duke_0066D_11593.pdf (accessed 29/07/2014).

²⁷ J.R. Giska, MSc Thesis, Oregon State University, 2013; http://ir.library.oregonstate.edu/xmlui/bitstream/handle/1957/39835/GiskaJon_athanR2013.pdf (accessed 29/07/2014).

²⁸ A.K. Suresh, D.A. Pelletier, M.J. Doktycz, *Nanoscale*, 2013, **5**, 463.

²⁹ R. Ma, C. Levard, S.M. Marinakos, Y. Cheng, J. Liu, F.M. Michel, G.E. Brown, G.V. Lowry, *Environ. Sci. Technol.*, 2012, **46**, 752.

³⁰ J. Liu, Z. Wang, F.D. Liu, A.B. Kane, R.H. Hurt, *ACS Nano* 2012, **6**, 9887.

³¹ J. Liu, R.H. Hurt, *Environ. Sci. Technol.* 2010, **44**, 2169.

³² L.R. Pokhrel, B. Dubey, P.R. Scheuerman, *Environ. Sci. Nano*, 2014, **1**, 45.

³³ N. Akaighe, R.I. MacCuspie, D.A. Navarro, D.S. Aga, S. Banerjee, M. Sohn, V.K. Sharma, *Environ. Sci. Technol.*, 2011, **45**, 3895.

³⁴ C. Levard, B.C. Reinsch, F.M. Michel, C. Oumahi, G.V. Lowry, G.E. Brown, *Environ. Sci. Technol.* 2011, **45**, 5260.

- ³⁵ R. Kaegi, A. Voegelin, C. Ort, B. Sinnet, B. Thalmann, J. Krismer, H. Hagedorfer, M. Elumelu, E. Mueller, *Water Res.* 2013, **47**, 3866.
- ³⁶ R. Ma, C. Levard, J.D. Judy, J.M. Unrine, M. Durenkamp, B. Martin, B. Jefferson, G.V. Lowry, *Environ. Sci. Technol.* 2014, **48**, 104.
- ³⁷ R. Ma, J. Stegemeier, C. Levard, J.G. Dale, C.W. Noack, T. Yang, G.E. Brown, G.V. Lowry, *Environ. Sci.: Nano*, 2014, **1**, 347.
- ³⁸ M.R. Chang, D.J. Lee, J.Y. Lai, *J. Env. Manage.*, 2007, **85**, 1009.
- ³⁹ H.P. Jarvie, H. Al-Obaidi, S.M. King, M.J. Bowes, M.J. Lawrence, A.F. Drake, M.A. Green, P.J. Dobson, *Environ. Sci. Tech.*, 2009, **43**, 8622; and accompanying Supporting Information.
- ⁴⁰ L.K. Limbach, R. Bereiter, E. Mueller, R. Krebs, R. Gaelli, W.J. Stark, *Environ. Sci. Technol.*, 2008, **42**, 5828.
- ⁴¹ M.A. Kiser, P. Westerhoff, T. Benn, Y. Wang, J. Pérez-Rivera, K. Hristovski, *Environ. Sci. Technol.*, 2009, **43**, 6757.
- ⁴² P. Westerhoff, G. Song, K. Hristovski, M.A. Kiser, *J. Environ. Monit.*, 2011, **13**, 1195.
- ⁴³ Y. Wang, P. Westerhoff, K.D. Hristovski, *J. Haz. Mater.*, 2012, **201–202**, 16.
- ⁴⁴ E. Lombi, E. Donner, E. Tavakkoli, T.W. Turney, R. Naidu, B.W. Miller, K.G. Scheckel, *Environ. Sci. Technol.*, 2012, **46**, 9089.
- ⁴⁵ R. Kaegi, A. Voegelin, B. Sinnet, S. Zuleeg, H. Hagedorfer, M. Burkhardt, H. Siegrist, *Environ. Sci. Technol.*, 2011, **45**, 3902.
- ⁴⁶ C.A. Impellitteri, S. Harmon, R.G. Silva, B.W. Miller, K.G. Scheckel, T.P. Luxton, D. Schupp, S. Panguluri, *Water Res.* 2013, **47**, 3878.
- ⁴⁷ C.L. Doolette, M.J. McLaughlin, J.K. Kirby, D.J. Batstone, H.H. Harris, H. Ge, G. Cornelis, *Chemistry Central Journal*, 2013, **7**, 46.
- ⁴⁸ L. Hou, K. Li, Y. Ding, Y. Li, J. Chen, X. Wu, X. Li, *Chemosphere*, 2012, **87**, 248.
- ⁴⁹ M. Tejamaya, I. Römer, R.C. Merrifield, J.R. Lead, *Environ. Sci. Technol.*, 2012, **46**, 7011.
- ⁵⁰ A.C. Johnson, M.D. Jurgens, A.J. Lawlor, I. Cisowska, R.J. Williams, *Chemosphere*, 2014, **112**, 49.
- ⁵¹ T. Maruejous, P. Lessard, B. Wipliez, G. Pelletier, P.A. Vanrolleghem, *Water Sci. Technol.* 2011, **64(9)**, 1898.
- ⁵² R.Y.G. Andoh, R.P.M. Smisson, *Water Sci. Technol.* 1996, **33(9)**, 127.
- ⁵³ J. Penfold, E. Staples, I. Tucker, R.K. Thomas, *Langmuir*, 2002, **18**, 5755.
- ⁵⁴ J. Penfold, E.J. Staples, I. Tucker, L.J. Thompson, *Langmuir*, 1997, **13**, 6638.
- ⁵⁵ J. Lyklema (Ed), *Fundamentals of Interface and Colloid Science, Volume IV: Particulate Colloids*, Academic Press, 2005.
- ⁵⁶ A.R. Whitley, C. Levard, E. Oostveen, P.M. Bertsch, C.J. Matocha, F.v.D.Kammer, J.M. Unrine, *Environ. Pollut.*, 2013, **182**, 141.
- ⁵⁷ H. Dong, I.M.C. Lo, *Water Res.*, 2013, **47**, 2489.
- ⁵⁸ http://soft-matter.seas.harvard.edu/index.php/Origins_of_surface_charge
- ⁵⁹ A. Carré, V. Lacarrière, *Contact Angle, Wettability and Adhesion*, Vol. 4, pp. 1–14, (Ed) K. L. Mittal, VSP/Brill 2006.
- ⁶⁰ X.-H. Zhou, B.-C. Huang, T. Zhou, Y.-C. Liu, H.-C. Shi, *Chemosphere*, 2015, **119**, 568.
- ⁶¹ J.E. Song, T. Phenrat, S. Marinakos, Y. Xiao, J. Liu, M.R. Wiesner, R.D. Tilton, G.V. Lowry, *Environ. Sci. Technol.*, 2011, **45**, 5988.
- ⁶² R. Aveyard, B.P. Binks, P.D.I. Fletcher, J.R. McNab, *Langmuir*, 1995, **11**, 2515.
- ⁶³ <http://www.isis.stfc.ac.uk/instruments/loq/>
- ⁶⁴ H.P. Jarvie, S.M. King, *Environ. Sci. Tech.* 2007, **41**, 2868; and accompanying Supporting Information.
- ⁶⁵ P. Carter, J. Worrell, G. Daigger, E. Allen, G. Land, *Proc. Water Environ. Fed.*, WEFTEC 2003 Sessions 21 – 30, 2003, **21**, 312.
- ⁶⁶ T. Pavón-Silva, V. Pacheco-Salazar, J.C. Sánchez-Meza, G. Roa-Morales, A. Colin-Cruz, *J. Environ. Sci. Health Part A*, 2009, **44**, 108.
- ⁶⁷ I. Bekri-Abbes, S. Bayouhd, M. Baklouti, *Desalination*, 2007, **204**, 198.
- ⁶⁸ A.S. Landim, G.R. Filho, R.M.N. de Assunção, *Polym. Bull.*, 2007, **58**, 457.
- ⁶⁹ U.S. Patent Number 5423990, 1995.
- ⁷⁰ R.K. Heenan, S.M. King, R. Osborn, H.B. Stanley, *Rutherford Appleton Laboratory Report*, 1989, RAL-89-128; S.M. King, R.K. Heenan, *Rutherford Appleton Laboratory Report*, 1995, RAL-95-005.
- ⁷¹ G.D. Wignall, F.S. Bates, *J. Appl. Crystallogr.*, 1987, **20**, 28.
- ⁷² <http://www.sasview.org/>
- ⁷³ S.M. King, H.P. Jarvie, *Environ. Sci. Technol.*, 2012, **46**, 6959; and accompanying Supporting Information.
- ⁷⁴ J. Teixeira, *J. Appl. Cryst.*, 1988, **21**, 781.
- ⁷⁵ J. Cai, N. Lu, C.M. Sorensen, *J. Coll. Int. Sci.*, 1995, **171**, 470.
- ⁷⁶ H. Lamb, *Hydrodynamics*. 6th Edition. Cambridge University Press, 1932. Reprinted 2006.
- ⁷⁷ A. Doostmohammadi, S. Dabiri, A.M. Ardekani, *J. Fluid Mech.*, 2014, **750**, 5.